Journal of Membrane Science 338 (2009) 75–83

Contents lists available at ScienceDirect

Journal of Membrane Science

journal homepage: www.elsevier.com/locate/memsci

Nafion®/H-ZSM-5 composite membranes with superior performance for direct methanol fuel cells

Mustafa Hakan Yildirim[a], Anna Roca Curoś[b], Julius Motuzas[c], Anne Julbe[c], Dimitrios F. Stamatialis[a,*], Matthias Wessling[a]

[a] Institute of Mechanics, Process and Control – Twente (IMPACT), University of Twente, Faculty of Science and Technology, Membrane Science and Technology, P.O. Box 217, 7500 AE Enschede, The Netherlands
[b] Chemical University of Barcelona, Chemical Engineering, C/Martí I Franqués 1, 08028, Barcelona, Spain
[c] Institut Européen des Membranes (UMR 5635 CNRS) University Montpellier 2, CC47 Place Eugène Bataillon, F-34095 Montpellier Cedex 5, France

ARTICLE INFO

Article history:
Received 29 September 2008
Received in revised form 6 April 2009
Accepted 7 April 2009
Available online 16 April 2009

Keywords:
Nafion
Zeolite
Methanol cross-over
Proton conductivity
Direct methanol fuel cell

ABSTRACT

Solution cast composite direct methanol fuel cell membranes (DEZ) based on DE2020 Nafion® dispersion and in-house prepared H-ZSM-5 zeolites with different Si/Al ratios were prepared and thoroughly characterized for direct methanol fuel cell (DMFC) applications.

All composite membranes have indeed lower methanol permeability and higher proton conductivity than pure DE2020 membrane. The composite membranes with Si/Al ratio 25 and 5 wt.% of zeolites (DEZ25-5) having the lowest methanol permeability and the membrane with Si/Al ratio 50 and 1 wt.% of zeolites (DEZ50-1) having the highest proton conductivity were tested in the DMFC for several days. The DEZ25-5 has the best performance; namely high power density and stable performance in time.

1. Introduction

Direct methanol fuel cells (DMFCs) gained attention recently as candidates for mobile power sources to portable electronic devices [1–5] due to their high energy density and easy and significantly fast charging times. To increase the proton conductivity and decrease the methanol cross-over of the electrolyte membrane, zeolites can be used. Zeolites have two important properties:

1. Very high water retention ability, which can only be eliminated at around 200 °C.
2. Molecular sieving properties, making them suitable for selective separations based on molecular size and shape [6–8].

Unfortunately, membranes made of pure zeolites are brittle, fragile and often have defects [9]. Composite membranes can be made using zeolites as fillers and a polymeric matrix as a host. If the zeolites are well dispersed in the matrix, they can serve as extra route for proton transport in the membrane in addition to the already existing water channels. This leads to increase of the membrane conductivity and at the same time, the tortuous pathway created by the zeolites can decrease the methanol cross-over.

DuPont's Nafion® is a good choice as a host material for the zeolites due to its excellent proton conductivity, mechanical strength and thermal and chemical stability [10–14]. In fact, researchers made already several attempts to prepare and characterize Nafion/zeolite composite membranes for DMFC applications [15–22]. In some cases the proton conductivity and methanol cross-over is reported without DMFC results [20–22]. The ratio of proton conductivity and methanol permeability (often indicated as "β") is then used to predict DMFC performance. As we showed in earlier study [23], very often β value has rather low predictive power. In other cases DMFC performances are reported, but for high temperature applications or for ambient systems [16–19]. In this study we are particularly interested in the preparation and characterization of Nafion/H-ZSM-5 composite membranes for DMFC. To the best of our knowledge: for those membranes there are no DMFC results reported in the literature although these composites seem to have promising properties [22]. Therefore, H-ZSM-5 zeolites with various Si/Al ratios are prepared in-house using microwaves-assisted heating. Then, they are incorporated into Nafion membranes at various loadings (1, 3 and 5 wt.%). All composite membranes are tested with respect to swelling degree, proton conductivity and methanol permeability. Selected membranes with the highest proton conductivity and lowest methanol cross-over are tested for several days in DMFC. For comparison, the performance of pure DE2020 (membrane prepared by solution cast method using DE2020 Nafion® dispersion) membranes

* Corresponding author. Tel.: +31 53 4894675; fax: +31 53 4894611.
E-mail address: d.stamatialis@utwente.nl (D.F. Stamatialis).

0376-7388/$ – see front matter © 2009 Elsevier B.V. All rights reserved.
doi:10.1016/j.memsci.2009.04.009

and also commercially available extruded Nafion 117 membranes are investigated.

2. Experimental

2.1. Materials

DE2020 Nafion® dispersion (20 wt.% Nafion® + 80 wt.% water and VOCs, 1000 equivalent weight (EW)) was purchased from Ion Power Inc. (U.S.A.). DMSO was purchased from Aldrich (Germany). E-TEK electrodes were purchased from E-TEK DeNora (U.S.A.). Aluminum sulfate hexadecanohydrate ($Al_2(SO_4)_3{\cdot}16H_2O$, 98%) and tetraethylorthosilicate (TEOS, 98%) was purchased from Aldrich. Tetrapropylammonium hydroxide (TPAOH, 20% aqueous solution) was purchased from Sigma.

2.2. Seeds synthesis

Polymer–zeolite composite membranes can be prepared using small zeolite crystals obtained by milling of big crystals. A precise control of the process parameters is needed for controlling crystal size and homogeneity. Besides, nanosized zeolite crystals can be prepared by hydrothermal synthesis, although long ageing times and/or durations are generally required for obtaining small and uniform crystal sizes by conventional heating methods [24,25]. Microwaves-assisted heating is an attractive strategy for reducing synthesis time and obtaining uniform nanocrystals [26].

In the present study microwave heating is used to prepare ZSM-5 nanosized crystals within a few hours, starting from sol with a Si/Al molar ratio in the range 25–100. Mother sols were prepared by mixing TEOS (98%), ultrapure water (18.2 MΩ) and TPAOH (20% aqueous solution). $Al_2(SO_4)_3{\cdot}16H_2O$ (98%) was used as Al precursor. The mother sol composition was: xAl_2O_3:1SiO_2:0.4TPAOH:19.5H_2O:4C_2H_5OH. The alumina concentration x was varied in the range 0.05–0.2 (Si/Al = 25–100) in the mother sol. Sols were aged at room temperature (25 °C) under stirring for 24 h in air. A sol quantity of about 20 g was used for each experiment. The microwave-assisted hydrothermal (MW-HT) synthesis of seeds was performed in two steps as reported by Motuzas et al. [26], using computer controlled Milestone ETHOS 1600 MW oven. The synthesis parameters have been chosen as follows: for the first step T_1 = 80 °C, t_1 = 90 min, P_1 = 250 W and for the second step T_2 = 160 °C, t_2 = 60 min, P_2 = 400 W. After synthesis, the suspensions were cooled to 50–60 °C and removed from the autoclave. This cooling step occurred by classical convection and lasted typically 30–40 min.

The solid product was separated from the liquid phase by centrifugation at 9500 rpm (JOUAN B4i), washed twice with distilled water and centrifuged in order to reach a neutral pH. The recovered solid product was dried for 4 h at 155 °C and calcined at 550 °C during 4 h with a slope up and down of 0.5 °C/min. The phase purity and dimensions of the calcined crystals were respectively characterized by X-ray diffraction and scanning electron microscopy.

2.3. Membrane preparation

A predetermined amount of zeolite was added to 10 g of DMSO and sonicated for 1–2 h in an ultrasonic bath to disperse the zeolite. Then 50 g of DE2020 Nafion® dispersion was added and mixed vigorously for 1 h. After that it was cast on Teflon plate with a casting knife and placed in the fumehood for 18 h. The obtained membrane was annealed at 150 °C for 1 h and then was peeled off from the Teflon plate. Membranes of dry thickness of 50 μm and with zeolite content of 1, 3 and 5 wt.% of the dry Nafion weight, were prepared.

Same method was followed to prepare pure DE2020 membranes, but this time no zeolite was added. Membranes were named as follows: DEZ X–Y, where DE, Z, X and Y stands for DE2020 Nafion, ZSM-5 zeolite, Si/Al ratio of the zeolite and the weight percentage of the zeolite, respectively (i.e. DEZ75-3 is DE2020 membrane containing 3 wt.% of ZSM-5 zeolite with the 75 Si/Al ratio).

2.4. Membrane characterization

2.4.1. Scanning electron microscopy (SEM)

Membranes were visualized by a scanning electron microscope (Jeol JSM 5600LV). The membrane samples were sputtered with a thin layer of gold (30 nm) using a Balzers Union SCD 040 sputtering device prior to the SEM observation.

2.4.2. Swelling degree (SD)

Membranes were dried in the vacuum oven at 30 °C for 1 day and then immersed in ultrapure water (25 °C). The weight of wet ($Weight_{wet}$) and dry ($Weight_{dry}$) samples were measured. The SD of the membrane was calculated using:

$$\mathrm{SD}(\%) = \left(\frac{Weight_{wet} - Weight_{dry}}{Weight_{dry}} \right) \times 100, \quad (1)$$

2.4.3. Methanol permeability

The methanol permeability, P [cm^2/s], at 25 °C was measured using a two compartment diffusion cell following the procedure described elsewhere [23].

2.4.4. Proton conductivity

Proton conductivity measurements were carried out at 25 °C and 100% relative humidity, in cells with two-probe configuration following the procedure described elsewhere [27]. Prior to all experiments, membranes were equilibrated in ultrapure water for 24 h.

2.5. Fabrication of membrane–electrode assemblies

E-TEK commercial electrodes were used to fabricate the membrane–electrode assemblies (MEAs). Both anode (Pt–Ru) and cathode (Pt) contain 5 mg/cm^2 of catalyst. The geometric area of each electrode was 6.25 cm^2. The MEAs were prepared by hot pressing of the anode and cathode on both sides of the membrane at 10 bar for 5 min at 125 °C.

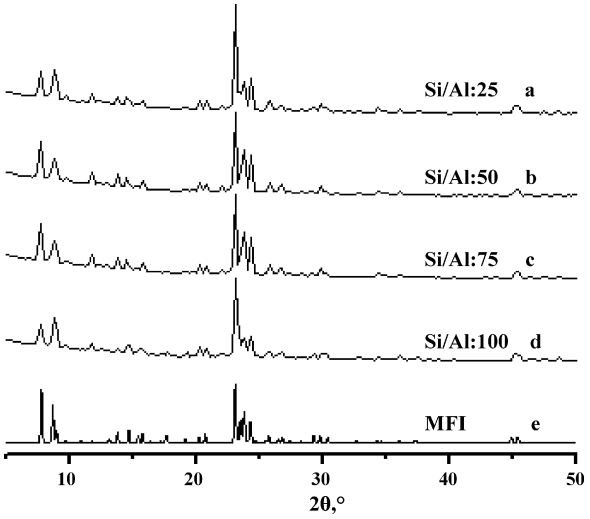

Fig. 1. XRD patterns of the MW-derived ZSM-5 crystals, prepared with different Si/Al molar ratios: (a) 25, (b) 50, (c) 75 and (d) 100. A MFI reference pattern is reported in (e) for comparison.

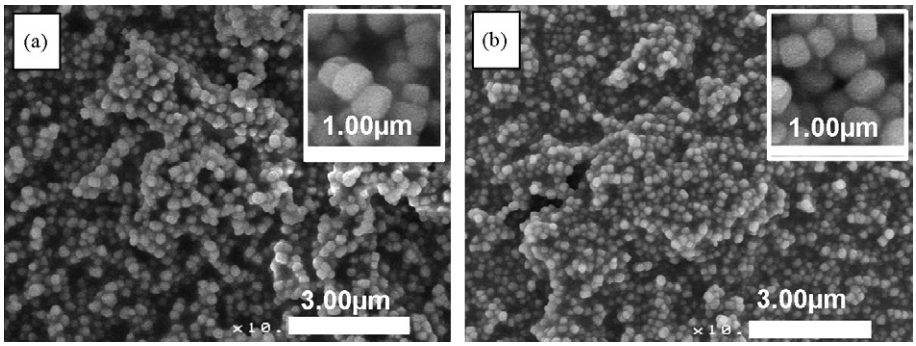

Fig. 2. SEM observations of the ZSM-5 crystals prepared by a two steps MW-assisted hydrothermal synthesis method (T_1 = 80 °C, t_1 = 90 min, P_1 = 250 W; T_2 = 160 °C, t_2 = 60 min, P_2 = 400 W) using different Si/Al molar ratios in the sol: (a) 25 and (b) 100.

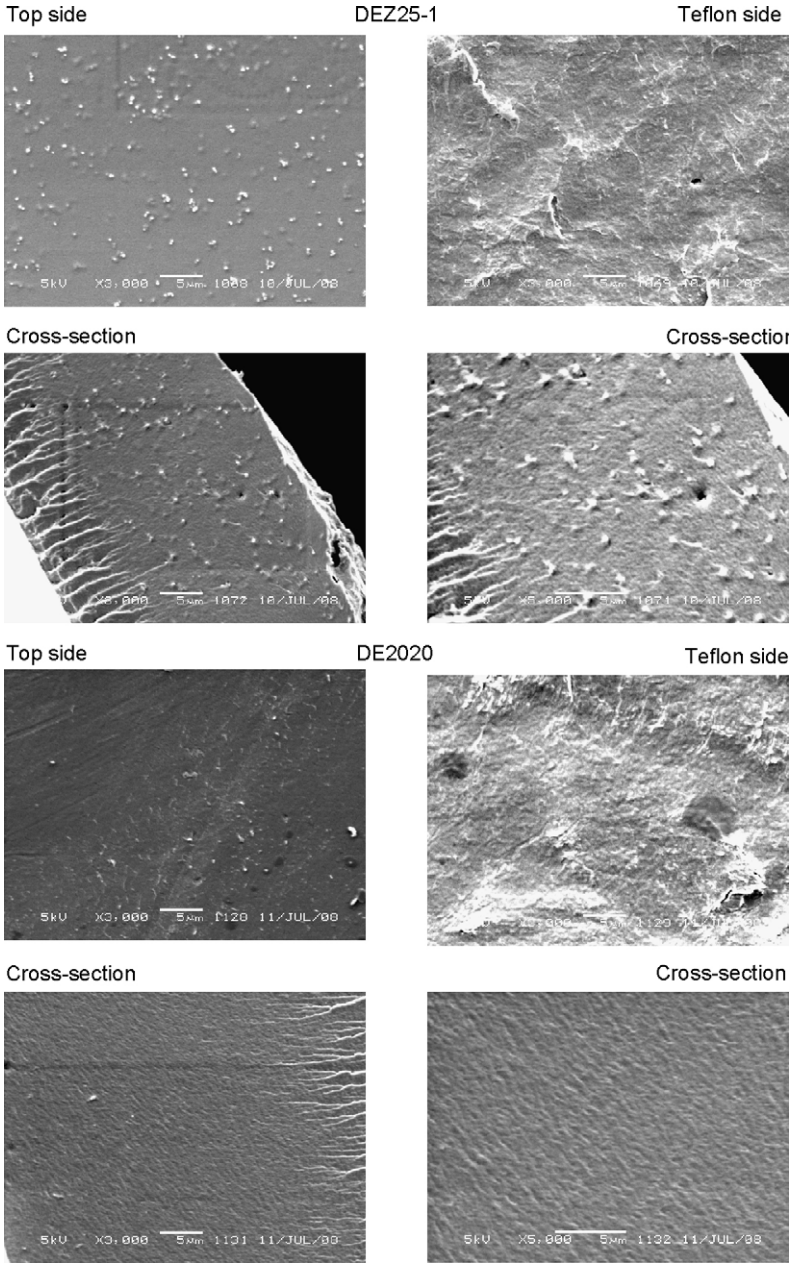

Fig. 3. SEM images of the DE2020 and the DEZ25-1 composite membrane.

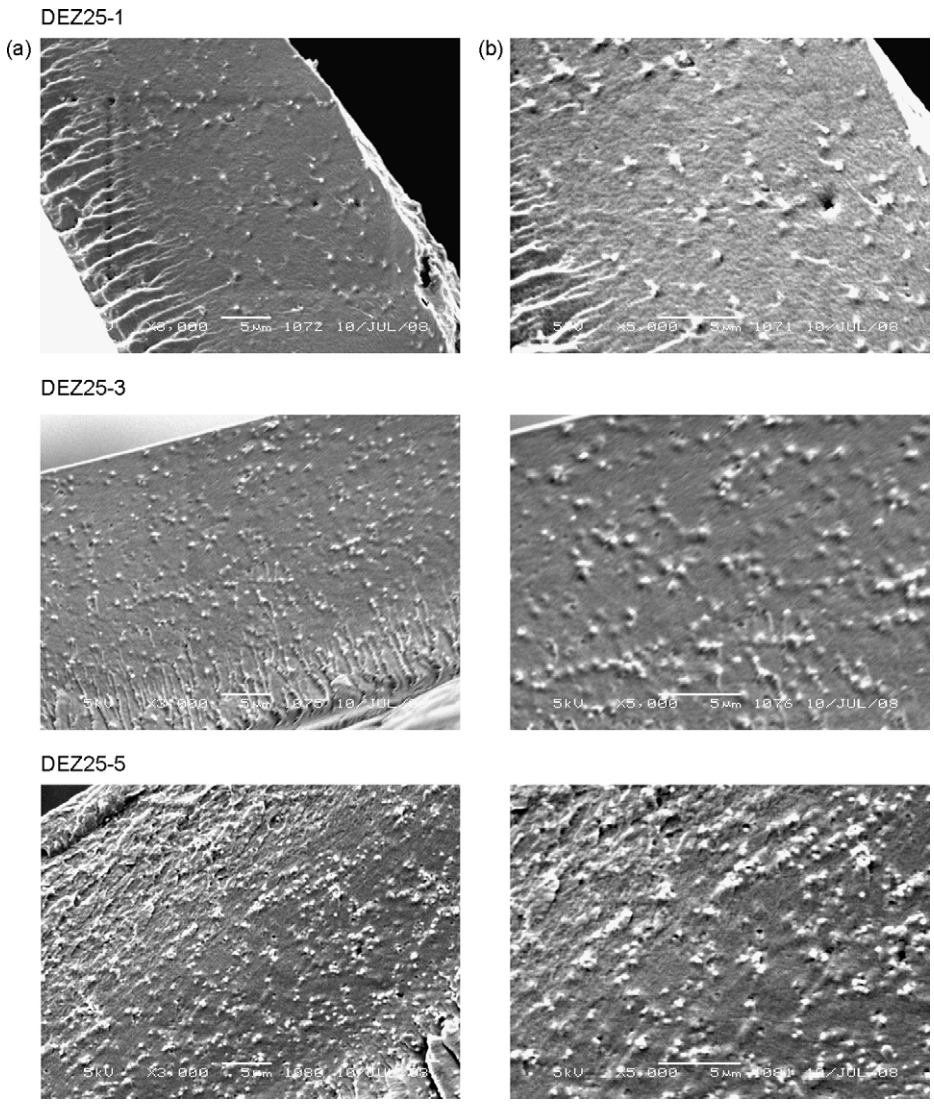

Fig. 4. Cross-section SEM images of the DEZ25-1, DEZ25-3 and DEZ25-5 composite membranes. (a) Magnification 3000× and (b) magnification 5000×.

2.6. Single cell DMFC performance

The DMFC performance of the MEAs was evaluated following the procedure described elsewhere [23]. The MEA was clamped between two graphite blocks. A serpentine flow pattern is etched in each of the graphite blocks to provide fuel to the MEA. 1 M methanol solution was fed to the anode at flow rates of 20 ml/min and dry oxygen was fed to the cathode at flow rates of 75 ml/min and back pressure of 2 bar. The temperature of the cell was kept at 80 °C.

3. Results and discussion

3.1. Characterization of the H-ZSM-5 zeolites

As shown in Fig. 1, independent from the Al concentration in the mother sol, well crystallized seeds with XRD patterns consistent with the MFI reference, were obtained after only 1 h synthesis at 160 °C.

Fig. 2 shows SEM images of the seeds. Although generally sols with increasing Al concentrations tend to yield bigger seeds, in our case very similar crystal sizes (in the range of 200–300 nm) were obtained independent from the Al content in the mother sol. Consequently the influence of ZSM-5 seed size on the derived composite membrane performance will be neglected in comparison with the influence of crystal hydrophilicity which strongly increases with the Al concentration.

3.2. SEM study of DE2020/ZSM-5 composite membranes

Fig. 3 shows typical SEM images of the surfaces and cross-section of DE2020 membrane and DEZ25-1 composite membrane. Top side of the composite membrane (facing the air) seems to be smoother and have more particles than the side facing Teflon plate probably due to the difference in hydrophilicity of zeolites and Teflon. Besides, the zeolite particles might be dragged to the surface of the membrane during solvent evaporation.

Cross-sections of the composite membrane show that the distribution of the zeolite particles is good probably due to the ultrasonication during the membrane preparation. Pure DE2020 membrane has no zeolites in it and has clear surface and cross-section SEM images.

Fig. 4 shows typical cross-section SEM images of the DEZ25-1, DEZ25-3 and DEZ25-5 composite membranes. Although aggregation might occur for DEZ25-5 membrane, the dispersion of the zeolite particles inside the membrane looks good. There is no visible accumulation of the zeolites towards any of the sides. Similar phenomena have been observed for the other composite membranes, as well.

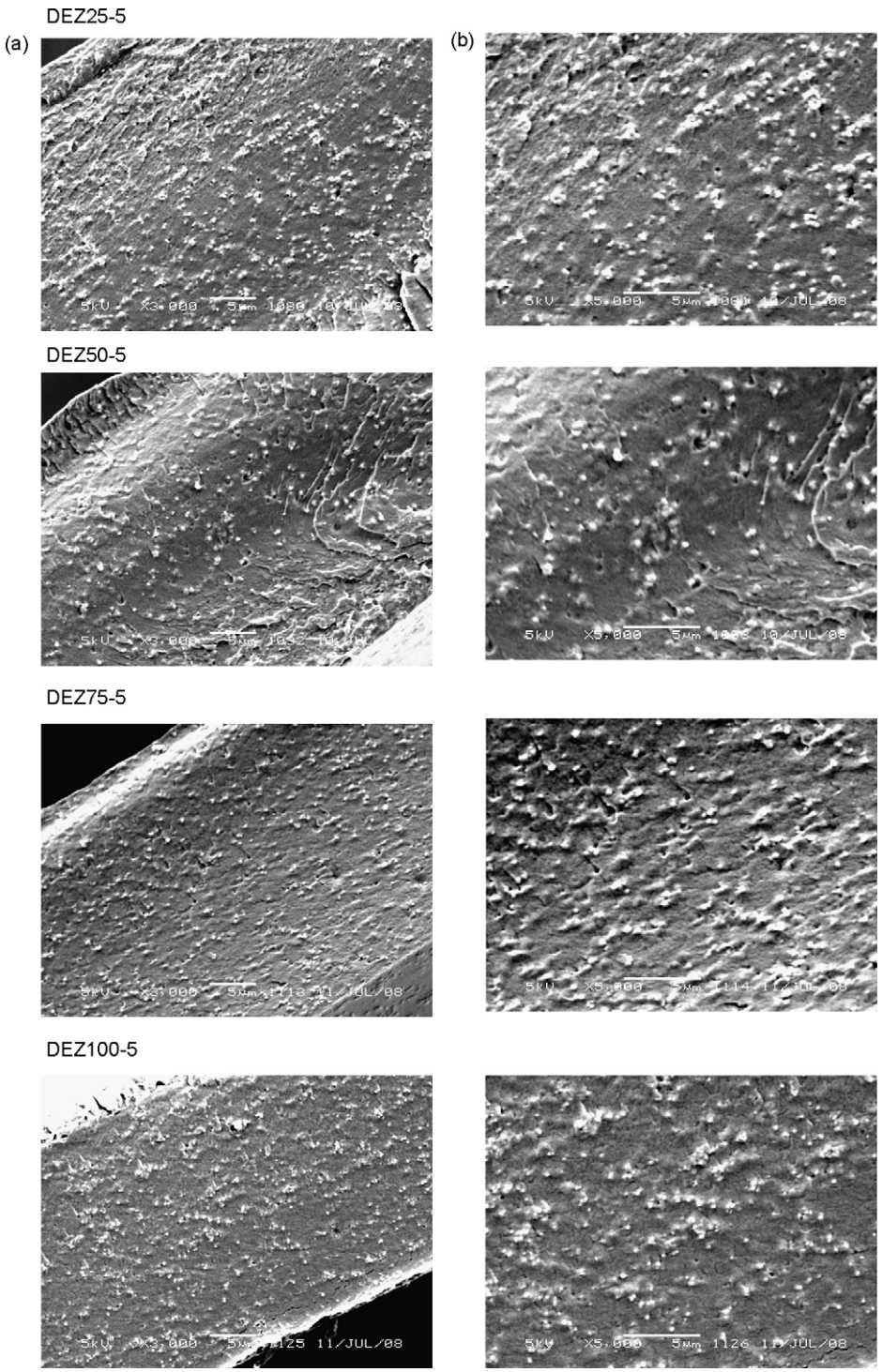

Fig. 5. Cross-section SEM images of the DEZ25-5, DEZ50-5, DEZ75-5 and DEZ100-5 composite membranes. (a) Magnification 3000× and (b) magnification 5000×.

Fig. 5 shows typical cross-section SEM images of the composites with the highest zeolite loading (DEZ25-5, DEZ50-5, DEZ75-5 and DEZ100-5). All composite membranes have similar SEM images, no accumulation of the zeolites at the top or the bottom side of the membranes.

3.3. Swelling experiments

Fig. 6 shows the swelling degrees of the membranes in ultrapure water. All composite membranes swell similar to DE2020 membrane. The difference in hydrophobicity of the zeolites (this increase in the order DEZ100 > DEZ75 > DEZ50 > DEZ25) does not seem to have a significant effect on the membrane swelling in ultrapure water.

3.4. Methanol permeability

Fig. 7a shows that the methanol permeabilities of the composite membranes are lower than pure DE2020 membrane, consistent with earlier study of Byun et al. [22] with Nafion/H-ZSM-5 compos-

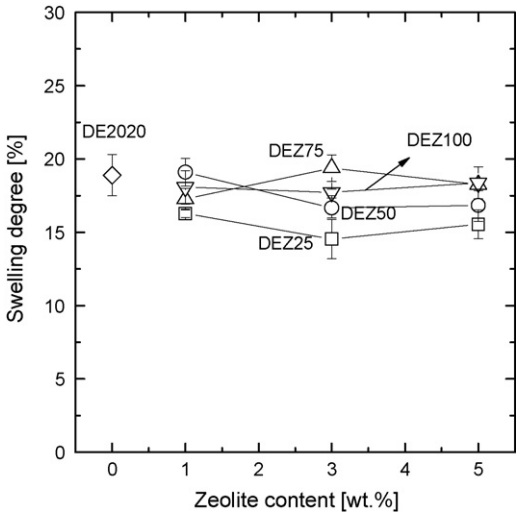

Fig. 6. Swelling degrees of DE2020 and DEZ membranes as a function of zeolite content.

ite membrane (Si/Al = 28). For most of the composite membranes, there is no effect of zeolite content or composition to the methanol cross-over. Interestingly, the methanol permeability of the DEZ25-5 is significantly lower than the others.

In the literature, Maxwell model is often used to describe transport properties in heterogeneous polymer systems. The simple form of Maxwell analyzes the steady-state dielectric properties of a dilute suspension of spheres where the permeability of a composite, *P*, made by dispersing of nonporous, impermeable filler in a continuous polymer matrix is expressed as

$$P = P_{\mathrm{P}} \times \left(\frac{1 - \varphi_{\mathrm{f}}}{1 + (\varphi_{\mathrm{f}}/2)} \right), \tag{2}$$

where P_{p} is the permeability of the pure polymer and φ_{f} is the volume fraction of filler. Eq. (2) suggests that the permeability of the filled polymer is lower than of the pure polymer and decreases with increasing of filler concentration. The decreased permeability is the result of a reduction in penetrant solubility due to (i) the replacement of polymer through which transport may occur with filler particles and (ii) an increase in tortuosity of the diffusion path through which the penetrant molecules cross the polymeric film [28].

Fig. 7b and c compares the experimental permeability results of two of the composite membranes (DEZ25 and DEZ50) with the theoretical prediction of a simple Maxwell model. The simple Maxwell model obviously fails to predict the experimental results, which are much lower than this prediction. Often aggregation of the particles, or phase separation occurs, causing significant change in the membrane morphology in comparison to pure polymer [28]. Besides, the morphology of the interface between the filler and polymer can be a critical determination of the overall transport properties [29]. Perhaps there is a rigidified polymer layer around the filler causing decrease in the permeability of the methanol through the composite membrane. The low cross-over of the DEZ25-5 membrane may be due to rigidification of the polymer around the particle in conjunction with particle aggregation.

3.5. Proton conductivity

Fig. 8 presents the proton conductivities of DE2020 and DEZ membranes as a function of zeolite content. Proton conductivi-

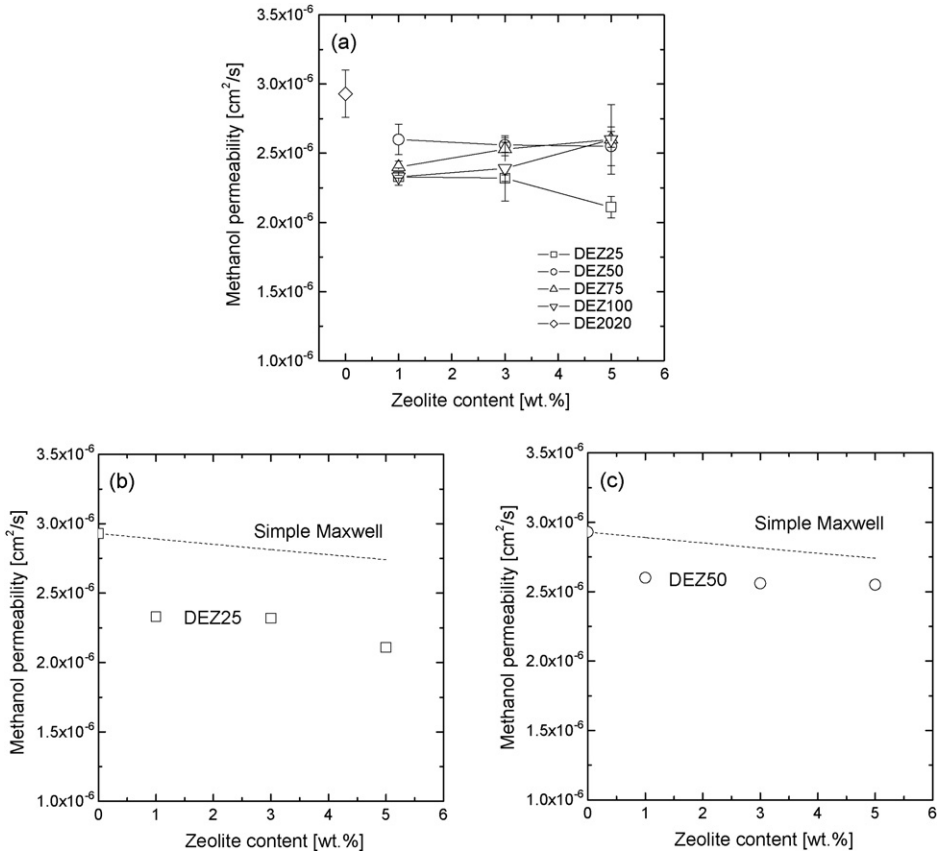

Fig. 7. Methanol permeabilities of DE2020 and DEZ membranes as a function of zeolite content. The dashed line represents the prediction of simple Maxwell model.

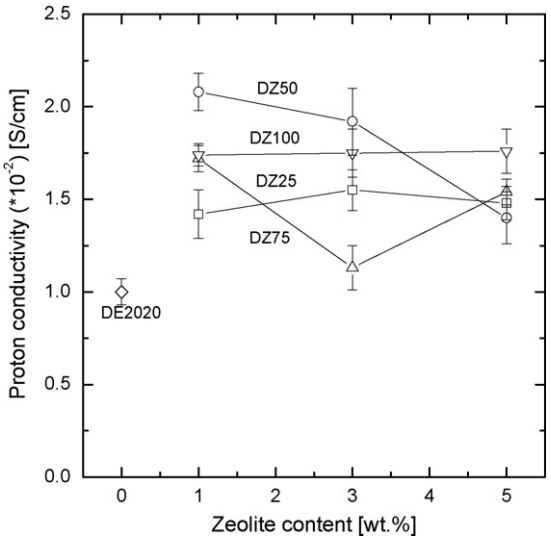

Fig. 8. Proton conductivities of DE2020 and DEZ membranes as a function of zeolite content.

ties of all composite membranes are higher than the pure DE2020 membrane, consistent with earlier study [22]. DEZ50-1 shows the highest proton conductivity among the DEZ50 membranes while the conductivities of DEZ25 and DEZ100 do not change significantly with the zeolite content. On the other hand, the conductivity of DEZ75 somewhat scatters with zeolite content in the membrane.

3.6. Single cell performance

In literature [8,20–22] studies, which are dealing with polymer–zeolite composite membranes for DMFCs, use the characteristic number, β (proton conductivity/methanol permeability), for prediction of DMFC performance instead of the real fuel cell. In this study, we combine the regular characterization methods with DMFC measurements. The DEZ25-5 and DEZ50-1 composite membranes were selected for further tests in DMFC due to their low methanol cross-over and high proton conductivity, respectively. Their performance is compared to that of pure DE2020. MEAs were prepared by hot pressing two E-TEK commercial electrodes on both sides of the membranes at 10 bar. At least two MEAs were prepared and measured for each type of membrane. Every day minimum 20 polarization curves (approximately 7 h of effective operation time per day) made for each MEA and then the system switched off and no methanol and oxygen fed to the system. The next day the system was switched on again and another 20 polarization curves were obtained. This procedure was followed for 5 days.

Fig. 9 presents typical results of maximum power density of each polarization curve as a function of time for DE2020, DEZ50-1, DEZ25-5 and N117 membranes. The concentration of methanol at the anode side was 1 M. Each symbol in the graphs corresponds to a different MEA. All three composite membranes show an increase in their maximum power density (MPD) up to 400th min. It seems that in the beginning of the experiment, maximum power densities increase due to the activation of all catalyst particles and also due to wetting of the membrane. The MPD of DE2020 membrane increases in the beginning of the measurement and then decreases continuously till the end of the measurement of the day. Next day, it again shows high MPD value and then decreases again and if one waits

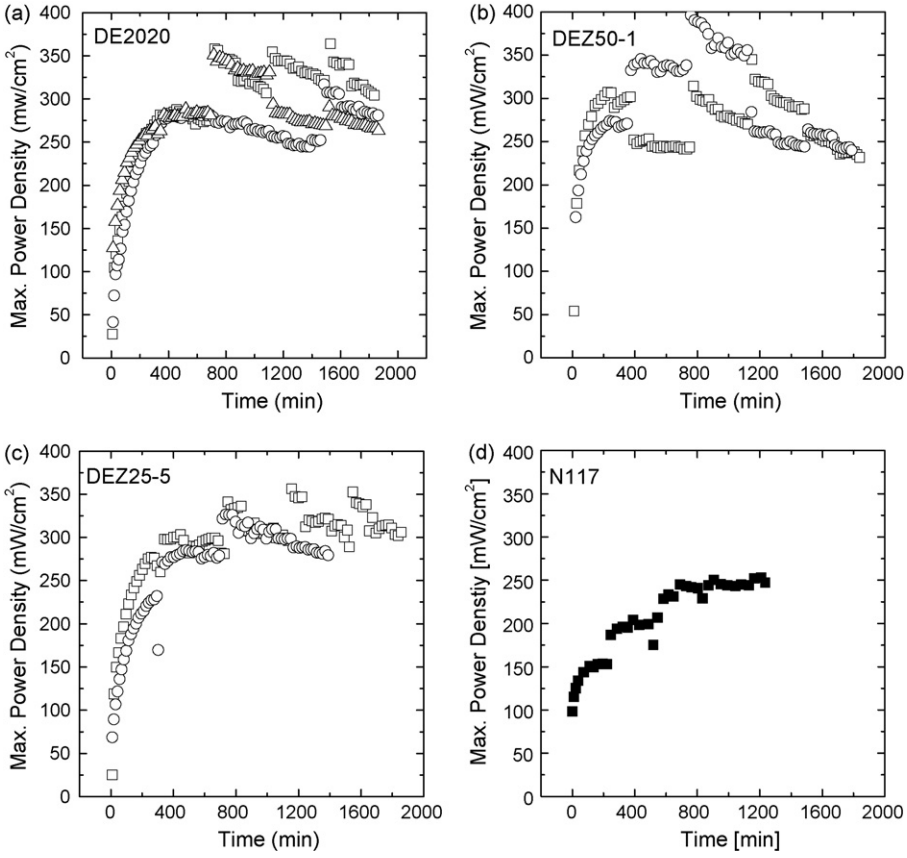

Fig. 9. Maximum power densities of (a) DE2020, (b) DEZ50-1, (c) DEZ25-5 and (d) N117 membranes [23] as a function of time (approximately 7 h of effective operation time per day). The different symbols in each case correspond to a different MEA.

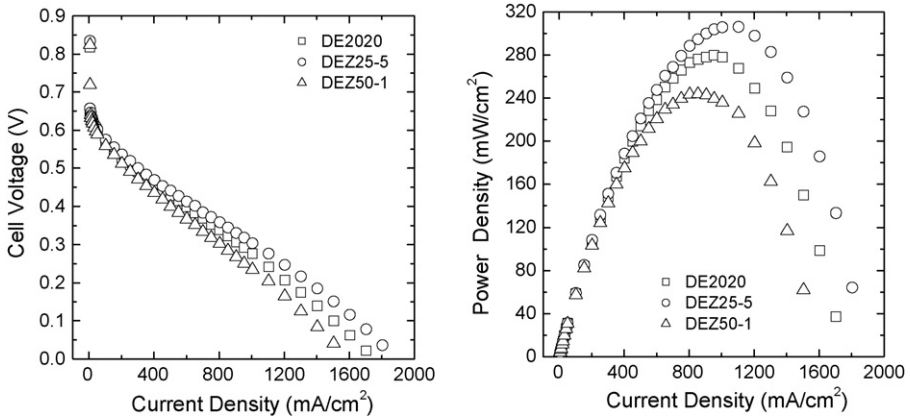

Fig. 10. Typical (a) polarization and (b) power density curves of DE2020, DEZ50-1 and DEZ25-5 membranes on the 5th measurement day in the DMFC.

long enough (4–5 days), MPD reaches around 275 mW/cm^2 (Fig. 9a), which is in agreement with our previous study for DE2020 membrane [23]. DEZ50-1 shows similar phenomena, perhaps, due to its low zeolite loading. Its MPD reaches 250–275 mW/cm^2 in the 5th day (Fig. 9b). The DEZ25-5 shows same trends; namely high MPD in the beginning of the day and drop later like the other two membranes. However, the drop is less sharp than the other two and most importantly reaches high MPD in the end of the 5th day at around 300 mW/cm^2. The performance of N117 MEA (taken from our earlier work [23], prepared under the same conditions as DEZ MEAs) is very stable without drop throughout the day (Fig. 9d). It seems that those fluctuations are characteristic of the specific DE2020 material and can be improved when significant amount (5 wt.%) of H-ZSM-5 is added.

Fig. 10 compares typical polarization and power density curves of the membranes in the end of the 5th day. In the polarization curves, there are clear regions of activation, ohmic and concentration polarization. Open cell voltages of all membranes are in the same range and they are about 0.85 V. The DEZ25-5 composite membrane with the lowest methanol crossover shows the best performance. This is shown clearly at the power density curves (Fig. 10b). DEZ25-5 composite membrane shows better performance than DE2020 and DEZ50-1 membranes at low and high current density regions.

Our results for the composite membranes suggest that the methanol cross-over is more critical to achieve superior DMFC performance. This is consistent with our earlier work for Nafion-PE (N-PE) composite membrane [23]. N-PE with lower methanol crossover than Nafion shows better DMFC performance even though it has lower proton conductivity than Nafion.

4. Conclusions

In this study, composite membranes were prepared by mixing H-ZSM-5 zeolites with DE2020 dispersion and thoroughly characterized. All composite membranes have lower methanol permeabilities and higher proton conductivities than pure DE2020 membrane. Two of the membranes: DEZ25-5 and DEZ50-1 were tested in DMFC due to their low methanol cross-over and high proton conductivity, respectively. The DEZ25-5 membrane showed the best DMFC results. Its maximum power density was more stable throughout the measurements and it reached the highest MPD at the end of the 5th day.

Acknowledgements

This research was financially supported by the Dutch Technology Foundation STW (Project no: 5713). The authors wish to thank:

- Dr. Gijs Calis (DSM Solutech, The Netherlands), Dr. Bernd Bauer (FumaTech GmbH, Germany) and Dr. Ronald Mallant (ECN, The Netherlands) for discussions and suggestions concerning this work.
- Dr. Suzana Pereira Nunes and Dr. Mauricio Schieda (Department of Membranes for Energy, GKSS Research Centre Geesthacht GmbH, Germany) for offering their proton conductivity set-up for our measurements.

References

[1] A. Blum, T. Duvdevani, M. Philosoph, N. Rudoy, E. Peled, Water-neutral micro direct-methanol fuel cell (DMFC) for portable applications, Journal of Power Sources 117 (1–2) (2003) 22.
[2] A. Simoglou, P. Argyropoulos, E.B. Martin, K. Scott, A.J. Morris, W.M. Taama, Dynamic modelling of the voltage response of direct methanol fuel cells and stacks. Part I. Model development and validation, Chemical Engineering Science 56 (23) (2001) 6761.
[3] C.Y. Chen, P. Yang, Performance of an air-breathing direct methanol fuel cell, Journal of Power Sources 123 (1) (2003) 37.
[4] S. Surampudi, S.R. Narayanan, E. Vamos, H. Frank, G. Halpert, A. LaConti, J. Kosek, G.K.S. Prakash, G.A. Olah, Advances in direct oxidation methanol fuel cells, Journal of Power Sources 47 (3) (1994) 377.
[5] S.C. Kelly, G.A. Deluga, W.H. Smyrl, A miniature methanol/air polymer electrolyte fuel cell, Electrochemical Solid-State Letters 3 (2000) 407.
[6] T.C. Bowen, R.D. Noble, J.L. Falconer, Fundamentals and applications of pervaporation through zeolite membranes, Journal of Membrane Science 245 (1–2) (2004) 1.
[7] Z. Huang, H.-M. Guan, W.I. Tan, X.-Y. Qiao, S. Kulprathipanja, Pervaporation study of aqueous ethanol solution through zeolite-incorporated multilayer poly(vinyl alcohol) membranes: effect of zeolites, Journal of Membrane Science 276 (1-2) (2006) 260.
[8] B. Libby, W.H. Smyrl, E.L. Cussler, Polymer-zeolite composite membranes for direct methanol fuel cells, AIChE Journal 49 (4) (2003) 991.
[9] M.B. Berry, B.E. Libby, K. Rose, K.H. Haas, R.W. Thompson, Incorporation of zeolites into composite matrices, Microporous and Mesoporous Materials 39 (1–2) (2000) 205.
[10] P.C. Rieke, N.E. Vanderborgh, Temperature dependence of water content and proton conductivity in polyperfluorosulfonic acid membranes, Journal of Membrane Science 32 (2–3) (1987) 313.
[11] G. Scibona, C. Fabiani, B. Scuppa, Electrochemical behaviour of nafion type membrane, Journal of Membrane Science 16 (1983) 37.
[12] W.Y. Hsu, J.R. Barkley, P. Meakin, Ion percolation and insulator-to-conductor transition in nafion perfluorosulfonic acid membranes, Macromolecules 13 (1) (1980) 198–200.
[13] N. Vanderborgh, T.V. Nguyen, The rate of isothermal hydration of polyperfluorosulfonic acid membranes, Journal of Membrane Science 143 (1998) 235.
[14] H.L. Yeager, R.S. Yeo, Structural and transport properties of perfluorinated ion-exchange membrane, Modern Aspects of Electrochemistry 16 (1985) 437.
[15] Z. Chen, B. Holmberg, W. Li, X. Wang, W. Deng, R. Munoz, Y. Yan, Nafion/zeolite nanocomposite membrane by in situ crystallization for a direct methanol fuel cell, Chemistry of Materials 18 (24) (2006) 5669.
[16] Y. Kim, J.S. Lee, C.H. Rhee, H.K. Kim, H. Chang, Montmorillonite functionalized with perfluorinated sulfonic acid for proton-conducting organic–inorganic composite membranes, Journal of Power Sources 162 (1) (2006) 180.
[17] V. Baglio, A.S. Arico, A. Di Blasi, P.L. Antonucci, F. Nannetti, V. Tricoli, V. Antonucci, Zeolite-based composite membranes for high temperature direct methanol fuel cells, Journal of Applied Electrochemistry 35 (2) (2005) 207.

[18] V. Baglio, A. Di Blasi, A.S. Arico, V. Antonucci, P.L. Antonucci, F. Nannetti, V. Tricoli, Investigation of the electrochemical behaviour in DMFCs of chabazite and clinoptilolite-based composite membranes, Electrochimica Acta 50 (2005) 5181.
[19] D.H. Jung, S.Y. Cho, D.H. Peck, D.R. Shin, J.S. Kim, Preparation and performance of a Nafion®/montmorillonite nanocomposite membrane for direct methanol fuel cell, Journal of Power Sources 118 (1–2) (2003) 205.
[20] E.N. Gribov, E.V. Parkhomchuk, I.M. Krivobokov, J.A. Darr, A.G. Okunev, Supercritical CO_2 assisted synthesis of highly selective nafion–zeolite nanocomposite membranes for direct methanol fuel cells, Journal of Membrane Science 297 (1–2) (2007) 1.
[21] J. Wang, X. Zheng, H. Wu, B. Zheng, Z. Jiang, X. Hao, B. Wang, Effect of zeolites on chitosan/zeolite hybrid membranes for direct methanol fuel cell, Journal of Power Sources 178 (1) (2008) 9.
[22] S.C. Byun, Y.J. Jeong, J.W. Park, S.D. Kim, H.Y. Ha, W.J. Kim, Effect of solvent and crystal size on the selectivity of ZSM-5/Nafion composite membranes fabricated by solution-casting method, Solid State Ionics 177 (37–38) (2006) 3233.
[23] M.H. Yildirim, D. Stamatialis, M. Wessling, Dimensionally stable Nafion–polyethylene composite membranes for direct methanol fuel cell applications, Journal of Membrane Science 321 (2) (2008) 364.
[24] S.B. Tantekin-Ersolmaz, Ç. Atalay-Oral, M. Tatller, A. Erdem-Senatalar, B. Schoeman, J. Sterte, Effect of zeolite particle size on the performance of polymer-zeolite mixed matrix membranes, Journal of Membrane Science 175 (2) (2000) 285.
[25] Q. Li, B. Mihailova, D. Creaser, J. Sterte, The nucleation period for crystallization of colloidal TPA-silicalite-1 with varying silica source, Microporous and Mesoporous Materials 40 (1–3) (2000) 53.
[26] J. Motuzas, A. Julbe, R.D. Noble, C. Guizard, Z.J. Beresnevicius, D. Cot, Rapid synthesis of silicalite-1 seeds by microwave assisted hydrothermal treatment, Microporous and Mesoporous Materials 80 (1–3) (2005) 73.
[27] D. Gomes, J. Roeder, M.L. Ponce, S.P. Nunes, Characterization of partially sulfonated polyoxadiazoles and oxadiazole–triazole copolymers, Journal of Membrane Science 295 (1–2) (2007) 121.
[28] D.M. Sterescu, D.F. Stamatialis, E. Mendes, M. Wubbenhorst, M. Wessling, Fullerene-modified poly(2,6-dimethyl-1,4-phenylene oxide) gas separation membranes: why binding is better than dispersing, Macromolecules 39 (26) (2006) 9234–9242.
[29] T.T. Moore, W.J. Koros, Non-ideal effects in organic–inorganic materials for gas separation membranes, Journal of Molecular Structure 739 (1–3) (2005) 87.